

## **Spatial targeting of infectious disease control: Identifying multiple, unknown sources**

Verity, R; Stevenson, MD; Rossmo, DK; Nichols, RA; Le Comber, SC

For additional information about this publication click this link.

<http://onlinelibrary.wiley.com/doi/10.1111/2041-210X.12190/abstract>

Information about this research object was correct at the time of download; we occasionally make corrections to records, please therefore check the published record when citing. For more information contact [scholarlycommunications@qmul.ac.uk](mailto:scholarlycommunications@qmul.ac.uk)

1 **Spatial targeting of infectious disease control: identifying multiple, unknown sources**

2

3 Robert Verity<sup>1\*</sup>, Mark D. Stevenson<sup>1\*</sup>, D. Kim Rossmo<sup>2</sup>, Richard A. Nichols<sup>1</sup>, Steven C. Le Comber<sup>1†</sup>

4

5 <sup>1</sup>School of Biological and Chemical Sciences, Queen Mary University of London, Mile End Road, London E1 4NS,

6 United Kingdom; and <sup>2</sup>Center for Geospatial Intelligence and Investigation, School of Criminal Justice, Texas State

7 University, 601 University Drive, San Marcos, TX 78666

8

9 \*These authors contributed equally to this paper,

10 †Correspondence author. E-mail: s.c.lecomber@qmul.ac.uk

11

12

13

14

15

16

17

18

## 19 **Summary**

20

21 **1.** Geographic profiling (GP) was originally developed as an analytical tool in criminology, where it uses the spatial  
22 locations of linked crimes (for example murder, rape or arson) to identify areas that are most likely to include the  
23 offender's residence. The technique has been extremely successful in this field, and is now widely used by police  
24 forces and investigative agencies around the world. More recently, the same method has been applied to biological  
25 data, notably in spatial epidemiology, where it uses the locations of disease cases to identify infection sources: the  
26 identification of these sources is critical to control efforts of diseases such as malaria, since targeted intervention is  
27 more efficient and cost effective than untargeted intervention.

28 **2.** Here we solve the problem of identifying multiple sources, even when the number of sources is unknown – a  
29 requirement for many biological studies. We present a new, rigorous mathematical and computational method, and  
30 show why previous Bayesian methods were often outperformed by the empirically-developed Criminal Geographic  
31 Targeting (CGT) algorithm used in criminology.

32 **3.** We use simulations and real-world examples to compare our model to both the CGT algorithm and to an existing  
33 Bayesian model. We demonstrate that our method combines the advantages of both previous methods, particularly  
34 in cases featuring large data sets and multiple sources.

35 **4.** Our approach provides an increase in search efficiency over other methods and is likely to lead to improved  
36 targeting of interventions and more efficient use of resources. We suggest that the Dirichlet process mixture (DPM)  
37 model provides a useful and practical tool for conservation biologists and epidemiologists that can be used to inform  
38 management decisions and public health policy.

39

## 40 **Keywords**

41 Bayesian statistics, criminology, Dirichlet process mixture, epidemiology, geographic profiling

42

## 43 **Abbreviations**

44 GP, geographic profiling; DPM, Dirichlet process mixture; MCMC, Markov Chain Monte Carlo

45

## 46 **Introduction**

47 In many areas of biology (for example invasion biology and epidemiology), models describing the ways in which  
48 animals, plants or pathogens spread outwards from a central source are of considerable importance. Such models are  
49 routinely used to generate risk maps in epidemiology, or to predict the effect of global climate change on the spread  
50 of invasive species (Kolar & Lodge 2001). Surprisingly, very few models exist which run backwards in time, using  
51 current spatial patterns to identify sources of infections or biological invasions, despite the fact that the identification  
52 of these sources can be used to target control efforts, dramatically improving the efficiency of interventions.

53 Recently, geographic profiling (GP) – a technique originally developed in criminology to help prioritise large lists of  
54 suspects in cases of serial crime (Rossmo, 2000) – has been successfully applied to biological data, providing a way  
55 of doing exactly this (Le Comber & Stevenson 2012).

56

57 Investigations of serial crime typically involve too many, rather than too few, suspects; for example, the  
58 investigation into the Yorkshire Ripper murders in the UK between 1975 and 1980 generated 268,000 names  
59 (Doney 1990). In criminology, GP techniques use spatial data concerning the locations of connected crime sites to  
60 create a surface of search priority that is overlaid on a map of the study area to produce a geoprofile, which in turn  
61 allows the police to prioritise investigations by systematically checking suspects associated with locations in  
62 descending order of the height on the geoprofile (Rossmo 2000). There are a number of different geographic  
63 profiling software programs available, including Rigel (Miller 2003), developed by Environmental Criminology  
64 Research Inc. (ECRI), CrimeStat (Levine 1996), funded by the U.S. National Institute of Justice, and Dragnet  
65 (Canter 2000), developed at the University of Liverpool. Other authors (for example Snook et al. (2002, 2005)) have  
66 made a case for the use of human judges. Of different programmes available, the most widely used is the criminal  
67 geographic targeting (CGT) algorithm of Rossmo (Rossmo 1993), which forms the basis of Rigel (Miller 2003), in  
68 which information from multiple crime sites is combined by means of summing over independent distributions. The  
69 CGT is used by organisations including the Royal Canadian Mounted Police, the Bureau of Alcohol, Tobacco,  
70 Firearms and Explosives, the Los Angeles Police Department, the National Crime Agency in the UK and the United  
71 States Marine Corps and has also been used to identify source populations during biological invasions and sources  
72 of infection during disease outbreaks (Le Comber et al. 2006; Raine et al. 2009; Le Comber et al. 2011; Stevenson et  
73 al. 2012).

74

75 The development of geographic profiling has – understandably – been driven by the need for practical solutions to  
76 the problems encountered by law enforcement agencies. O'Leary (O'Leary 2009; O'Leary 2010; O'Leary 2012)  
77 placed GP in a Bayesian framework, mathematically formalising the problem. However, the model put forward by  
78 O'Leary makes the simplifying assumption that all observed data points originate from a single source, and hence  
79 performs extremely badly in cases where there are actually multiple sources (see Methods and Results). Thus,  
80 despite the mathematical appeal of O'Leary's approach, the CGT algorithm continues to be widely used as a result of  
81 its proven track record (Rossmo 2000).

82

83 Here, we present a well-defined mathematical approach that unifies existing methods in a single framework.  
84 Crucially, our method explicitly deals with the issue of multiple sources – a situation typical of biological data sets,  
85 but less common in criminology. Under these circumstances, our model outperforms both the CGT algorithm and a  
86 simple Bayesian model based on the work of O'Leary (O'Leary 2010). Further, we develop a computational  
87 approach using Markov Chain Monte Carlo (MCMC) methods that extends the technique to large data problems.  
88 Finally, we demonstrate the effectiveness of our model using a real-life example of malaria cases in Egypt.

89

90 Specifically, we assert that (1) one of the reasons for the CGT algorithm's improved performance relative to the  
91 simple Bayesian model lies in its ability to deal with multiple sources; and hence by constructing a Bayesian model  
92 that incorporates the ability of the CGT algorithm to deal with multiple sources while maintaining the mathematical  
93 rigour of the simple Bayesian model, we can outperform both of the existing methods; (2) this method can be  
94 extended to large data problems using MCMC; (3) this method can be used to provide practical solutions to real-life  
95 problems, such as those found in epidemiology.

96

### 97 **Geographic Profiling Models**

98 The traditional (CGT) and Bayesian approaches to geographic profiling differ in both their construction and  
99 implementation. In the following sections we specify each in common terms.

100

### 101 **CGT algorithm**

102 The traditional method begins by considering a distance-decay function around each individual data point. The  
 103 height of the surface is a measure of how confident we are that the source location lies at this point. The decay  
 104 function can take a number of forms, but in criminological applications it is typical to use a two-part distribution that  
 105 increases to a maximum at a distance  $B$  from the data point, and then declines beyond this:

$$106 \quad f(d) = \begin{cases} \frac{1}{d^h}, & \text{if } d > B \\ \frac{kB^{g-h}}{(2B-d)^g}, & \text{if } d \leq B \end{cases} \quad [1]$$

107 where  $d$  is the distance (either Euclidian or Manhattan) from the observation. This distribution was originally  
 108 proposed by Rossmo (2000), but here we have used the notation of O'Leary (O'Leary 2009; O'Leary 2010)  
 109 (correcting for a mistake in the direction of the inequalities). In this paper we use the Euclidean distance throughout.  
 110 Although this decay function is often referred to as a probability distribution, this is not technically true as there is  
 111 no requirement for the surface to integrate to unity (nor, in criminology, any need for it to do so, since the analysis is  
 112 used to produce ranked scores rather than probabilities). Thus, in the traditional method the decay function is better  
 113 described as a surface of search priority, subject to the more general constraint that points high up on the surface  
 114 represent areas of high priority. This measure of priority is modelled as an additive quantity, meaning that the  
 115 information from several observations can be combined by summing together the independent surfaces. The end  
 116 result of this process of summation is a single surface that represents our integrated knowledge of the source  
 117 location, which is referred to as a jeopardy surface (Rossmo, 2000).

118

119 The search efficiency of the model can be calculated using the hit score percentage; the proportion of the area that  
 120 we must search before the true source location is found. The smaller the hit score percentage, the more accurate the  
 121 geoprofile, with a hit score percentage of 50% representing what we would expect from a non-prioritised random or  
 122 uniform search (see Rossmo 2000).

123

### 124 **Simple Bayesian model**

125 We compare the CGT algorithm against a simple Bayesian model based on the initial approach described by  
 126 O'Leary (O'Leary 2010; O'Leary 2012), and ignoring subsequent extensions relating to the choice of priors. This

127 approach differs from the CGT in that distributions are defined and manipulated according to the laws of  
128 probability. The starting point is to write down the probability of the data, given the known location of the source.  
129 This is achieved through the use of a probability distribution, which we will refer to as the migration profile, in  
130 which the probability of finding an observation at any point in the domain is expressed relative to the location of the  
131 source. Assuming independence between observations, the probability of the sample is simply the product over the  
132 probabilities of the individual data points (in fact, Rossmo (1995) considered a similar formulation in which the  
133 CGT algorithm is applied in log space). By placing a suitable prior on the source location and applying Bayes' rule it  
134 is possible to derive the posterior distribution of the source location, given the observations.

135

136 Unsurprisingly, the choice of method makes a big difference to the results. While the CGT algorithm tends to create  
137 a patchy distribution of peaks and troughs, entertaining the possibility of a number of different source locations, the  
138 simple Bayesian method tends to place the majority of the posterior probability mass around the spatial mean of the  
139 data points (at least for many choices of prior and likelihood, including those considered here). Another important  
140 difference between the methods is in the rate of convergence. In the Bayesian approach the variance of the posterior  
141 distribution tends to decrease rapidly as more data is added, whereas in the CGT method the variance of the  
142 geoprofile can never be less than the variance of the decay function. Generally, when there is in fact a single source  
143 location the Bayesian method is predicted to outperform the traditional method. However, if there is the potential for  
144 multiple source locations then the Bayesian method is predicted to converge quickly on the wrong answer, while the  
145 traditional method will still perform well. In this study, we test this prediction using a variety of simulations (see  
146 Results 1 and 2, below).

147

#### 148 **The Dirichlet process mixture model**

149 Our primary objective is to address the issue of multiple sources within a well-defined Bayesian framework. The  
150 tool that allows us to do this is the Dirichlet Process Mixture (DPM) model, which has a strong mathematical  
151 foundation (Ferguson 1983; Green & Richardson 2001) and is finding increasing application within biology (e.g.  
152 Huelsenbeck et al. 2006; Huelsenbeck & Andolfatto 2007; Dorazio et al. 2008). Unlike many clustering approaches,  
153 DPM models do not require the user to specify the number of clusters beforehand, making them extremely useful in  
154 situations where there is no strong prior information about the exact number of clusters. In place of a fixed number

155 of clusters, the DPM model describes the process of cluster formation using a single ‘concentration parameter’,  $\alpha$ .  
156 Specifically, if we have already seen  $n$  observations, of which  $n_A$  came from cluster  $A$ , then the (prior) probability of  
157 the next observation also belonging to cluster  $A$  is given by  $n_A/(n + \alpha)$ . It follows that, no matter how many  
158 observations we have seen, there is always a positive probability  $\alpha/(n + \alpha)$  of the next observation originating from a  
159 previously undiscovered cluster. While we may not believe there to be a truly unlimited number of clusters, by  
160 allowing for the possibility of an expanding number of clusters we can ensure that our model is always appropriate  
161 for the quantity of data at hand. Obviously the choice of the concentration parameter  $\alpha$  has a strong influence on the  
162 model. Although an appropriate value of  $\alpha$  could be fitted from training data, here we chose instead to integrate over  
163 our uncertainty by placing a diffuse hyper-prior over  $\alpha$  (of the form  $h(\alpha)=1/(1+\alpha)^2$ , see Appendix 2 for details).  
164 Where stronger prior information is available, the model can easily be adapted to include this.

165

166 The second part of the DPM model is the calculation of the posterior distribution of source locations, conditional on  
167 a particular partition of the data into clusters. This part is mathematically very similar to the simple Bayesian model,  
168 with the only difference being that a different posterior distribution is produced for each cluster. The likelihood of  
169 all observations in the same cluster is equal to the product of the migration profile over each of the observations. By  
170 incorporating an appropriate prior on the source location and applying Bayes’ rule we arrive at the posterior  
171 distribution of the source location from which this particular subset of observations derived. Carrying out this step  
172 for each cluster independently we obtain a set of posterior distributions – one for each of the (potentially) multiple  
173 source locations.

174

175 Finally, in order to obtain an analytical solution to the DPM model described above we would be required to sum  
176 over all possible partitions of the  $n$  data points into up to  $n$  clusters, weighted by the posterior probability of the  
177 partition in each case. The number of such partitions is given by the  $n^{\text{th}}$  Bell number ( $B_n$ ) which becomes  
178 prohibitively large for values as low as  $n=10$  ( $B_{10}=115,975$ ). Thus, for any reasonably sized data set we must turn to  
179 MCMC methods for a practical solution. Fortunately, a detailed exposition of MCMC algorithms for DPM models is  
180 provided by Neal (2000), and we need only to adapt these algorithms to our specific application. A more detailed  
181 description of the DPM model, including expressions relating to posterior inference under the analytical and MCMC  
182 forms of the solution, is provided in Appendices 1 to 3.



183

184 It is important to emphasise that the DPM model can be adapted to use any migration profile that satisfies the laws  
185 of probability (i.e. integrates to unity). The essence of the DPM model lies in the way that information is combined  
186 between clusters, and not in the specific details of the migration profile used. This can be seen in the logic of our  
187 study, which has four parts. (i) First, when comparing directly the CGT, simple Bayesian, and DPM models, we use  
188 the distribution from the CGT (described in equation [1]) as our migration profile in all three approaches. This  
189 ensures that the only difference between methods lies in the way that information is being combined, and not in any  
190 other assumptions relating to migration. (ii) Next, we validate the MCMC version of our proposed solution using  
191 this same migration profile, thereby ensuring that our MCMC results are directly comparable with our analytical  
192 results. (iii) From this, we move on to consider simulated data generated from a distribution more typical of those  
193 assumed in biology – the normal distribution – and explicitly compare the full form of the DPM model with the  
194 CGT under this assumption. (iv) Finally, we examine a real-world data set – an outbreak of malaria in Cairo – using  
195 all three models.

196

197

#### 198 **Methods(i) Comparing the simple Bayesian, CGT and DPM models**

199 As mentioned above, our first task is to compare the simple Bayesian, CGT and DPM models purely in terms of the  
200 way that information is combined in each case, and controlling for any differences between models, such as the  
201 migration profile. We simulated 6, 7, 8 or 9 data points from the distribution given in equation [1] ( $B=0.5$ ,  $f=4$ ,  $g=4$ ),  
202 emanating from either 1, 2 or 3 sources, truncated them to fit the available grid. For the purposes of simulation we  
203 split the domain into a  $100 \times 100$  grid, and replicated each combination of the number of data points and sources 1000  
204 times. Sources were chosen to fall within the central  $50 \times 50$  cells in a random, uniform manner. For each simulated  
205 data set we then used each of the three methods described above to search for the ‘unknown’ source locations, with  
206 search efficiency being measured in terms of the hit score percentage. The same distribution (distribution [1] with  
207  $B=0.5$ ,  $f=4$ ,  $g=4$ ) was used as the search distribution in each of the three methods. By designing simulations in this  
208 way we can capture an idealised situation in which all three methods make the same assumptions about the true  
209 dispersal distribution, and furthermore these assumptions are exactly correct (thereby removing another possible  
210 source of model error).

211

**212 (ii) MCMC validation**

213 For the reasons described previously, the analytical form of the DPM model can deal with only small data sets, and  
214 for larger data sets an MCMC implementation of the solution is required. For each of the 12000 simulations  
215 described above (1000 replicates of each combination of 1, 2 and 3 sources and 6, 7, 8 or 9 data points), we also  
216 used an MCMC implementation of the model, and calculated the correlation between the surface produced by the  
217 analytical form of the model and the MCMC form (see Appendix 3 for details of the MCMC algorithm). We also  
218 repeated the comparison of the DPM model with the CGT for larger data sets (1, 2 and 5 source locations; 20, 40,  
219 60, 80 and 100 spread points), using just the MCMC implementation of the model.

220

221 When running the MCMC, multiple chains were run simultaneously, with convergence being assessed using the  
222 Gelman-Rubin (GR) diagnostic statistic (Gelman et al. 2003) evaluated on the concentration parameter  $\alpha$  (using a  
223 value of GR=1.1 as a threshold for convergence). After the burn-in period, samples were obtained until the largest  
224 standard error of any point on the estimated surface was less than 0.01. Samples were not thinned, as it has  
225 previously been shown that this does not increase statistical power in situations such as this (Link & Eaton 2012).

226

**227 (iii) Further comparison of the CGT and DPM models**

228 The migration profile used above (distribution [1]) was designed for criminological applications. In some cases,  
229 including many biological applications, it may be more appropriate to assume alternative migration profiles. Here,  
230 we assume a bivariate normal migration profile, centred on the unknown source location(s), and with variance  $\sigma^2$ . In  
231 some cases, there will be biological data on dispersal patterns that can be used to inform the choice of  $\sigma$ ; for  
232 example, studies have shown that most malaria transmission occurs close to the larval breeding sites – usually  
233 between a few hundred meters and a kilometer– and rarely exceeds 2-3 km (Carter et al. 2000).

234

235 We are also required, as part of the DPM model, to choose a prior on the source location(s). For the sake of  
236 simplicity we use an empirical Bayes approach, assuming a bivariate normal prior, centred on the spatial mean of  
237 the observed data, and with variance  $\tau^2$ , where  $\tau$  was set to the maximum distance in either latitude or longitude

238 between the crime sites.  $\tau$  equals one standard deviation of the normal prior; hence, we expect our source to lie  
239 within this distance of the centre around two-thirds of the time, and the model allows for sources well outside the  
240 area bounding the crimes. Hence, there is a diffuse, non-informative prior over and beyond the normal search area.

241

242 We simulated 6, 7, 8 or 9 data points from a bivariate normal distribution with standard deviation  $\sigma = 1$  and  
243 emanating from either 1, 2 or 3 sources. For the purposes of simulation we split the domain into a  $100 \times 100$  grid, and  
244 replicated each combination of the number of data points and sources 1000 times. For each simulated data set we  
245 then used the two best performing methods described above (CGT and DPM) to search for the ‘unknown’ source  
246 locations, with search efficiency being measured in terms of the hit score percentage. The CGT uses the distribution  
247 describe in equation [1] with parameters fitted from the data as described by Rossmo (2000), while the DPM uses  
248 the spatial mean to fit  $\phi$ , with  $\sigma$  fixed at 1.

249

#### 250 **(iv) Case study**

251 We tested the performance of our model in a real world example by using the MCMC implementation of the DPM  
252 model to reanalyse data from Le Comber et al. (2011). In this study, spatial data relating to 139 recorded  
253 *Plasmodium vivax* malaria cases were collected, and buffer zones of 2 km were created around the locations of these  
254 malaria cases and merged to form a polygon of  $296.5 \text{ km}^2$  (Hassan 2006). All accessible aquatic habitats within this  
255 study area (surface/cryptic; temporary/semipermanent/permanent) were located and characterised between April and  
256 September 2005. These included water tanks, water pools created through pipelines or drainage system breakage,  
257 seepage from slum housing, natural springs, pools and ditches filled with ground water. Water sources included in  
258 this analysis were identified as bodies of water harbouring at least one mosquito larva over the study period ( $n = 59$ ).  
259 A total of 11 mosquito species were identified, including the malaria vectors *An. sergentii* and *An. pharoensis*, as  
260 well as other, non-vector, species. Of these 59 sites, seven tested positive for one or both of the malaria vectors *An.*  
261 *sergentii* and *An. pharoensis* (*An. sergentii* is well established as the most dangerous malaria vector in Egypt (Said  
262 et al. 1986)).

263

264 A dispersal distance of  $\sigma = 0.018$ , roughly corresponding to 1km, was used in the DPM model in  
265 correspondence with values in the literature (e.g. Carter et al. 2000) and a value of  $\tau = 0.328$  was fitted from the  
266 observed data (see above).

267

268 The model is written in R (R core team 2012) and integrates with Google Maps via the R package RgoogleMaps  
269 (Loecher 2012). The model used in this paper is available from the authors on request as an R package called  
270 'Rgeoprofile'.

271

272

## 273 **Results**

### 274 **(i) Comparing the simple Bayesian, CGT and DPM models**

275 Starting with the first set of simulations (1000 replicates of each combination of 1, 2 and 3 sources and 6, 7, 8 or 9  
276 data points), we used a fully factorial ANOVA to test the effect on the hit score percentage (or average hit score  
277 percentage when the number of sources was  $> 1$ ) of model type, number of sources and number of spread points.

278 Three model types were examined; the analytical form of the DPM model, the classical CGT algorithm and the  
279 simple Bayesian model.

280

281 Model type, number of points and number of sources all significantly affected the relative performance of the three

282 models (ANOVA: model type:  $F_{2,35964}=4787.05, p < 2e-16$ ; sources:  $F_{2,35964}=13099.30, p < 2e-16$ ; points:  $F_{3,$

283  $35964}=106.23, p < 2e-16$ ). All interactions were highly significant, with the  $F$  value for model type\*sources interaction

284 having the largest effect size ( $F_{4,35964}=2840.12, p < 2e-16$ ); none of the other  $F$  values exceeded 52. Tukey post-hoc

285 tests at  $\alpha=0.05$  showed that (1) the CGT significantly outperformed the simple Bayesian model, by an average of

286 1.81% (95% CI: 1.75-1.86%); (2) the DPM model showed a statistically significant improvement over both the CGT

287 algorithm, albeit only by 0.3% (95% CI: 0.25-0.36%) and the simple Bayesian model, again by about 2% (95% CI:

288 2.1-2.2%). Across all 12,000 runs, the DPM model performed better than the CGT in 68.2% of trials, and as well or

289 better in 74.9%, and better than the simple Bayesian model in 64.6% of trials, and as well or better in 91.5%.

290 However, although the DPM model outperformed the simple Bayesian model overall, the simple Bayesian model  
 291 had a small advantage when there was a single source (Figure 1).

292

### 293 **(ii) MCMC validation**

294 For the same simulated data sets described above we calculated the correlation between the surface produced by the  
 295 analytical form of the DPM model and the MCMC form. The two surfaces tended to extremely highly correlated ( $r$   
 296 (mean  $\pm$ sd) =  $0.9998 \pm 0.0010$ ), demonstrating that the MCMC algorithm does indeed find the same – or at least  
 297 extremely similar – posterior distributions as the analytical form of the model.

298

299 For the second set of simulations (1000 replicates of each combination of 1, 2 and 5 sources and 20, 40, 60, 80 or  
 300 100 data points) we performed the same analysis as in Results part 1, with extremely similar results (ANOVA:  
 301 model type:  $F_{1,29992}=167.7$ ,  $p<2e-16$ ; sources:  $F_{2,29992}=10603.1$ ,  $p<2e-16$ ; points:  $F_{4,29992}=1986.2$ ,  $p<2e-16$ ; model  
 302 type\*sources:  $F_{2,29992}=463.5$ ,  $p<2e-16$ ; model type\*points:  $F_{4,29992}=17.4$ ,  $p<2e-16$ ; sources\*points:  $F_{8,29992}=2916.7$ ,  
 303  $p<2e-16$ ; model type\*sources\*points:  $F_{8,29992}=0.9$ ,  $p=0.87$ ). Tukey post-hoc tests at  $\alpha=0.05$  showed that the DPM  
 304 model outperformed the CGT algorithm in a statistically significant way; again, this improvement was most marked  
 305 when the number of sources was  $> 1$  (Figure 2).

306

### 307 **(iii) Further comparison of the CGT and DPM models**

308 In the next set of simulations, in which a normal migration profile was assumed, we used ANOVA to test the effect  
 309 on the hit score percentage (or average hit score percentage when the number of sources was  $> 1$ ) of model type,  
 310 number of sources and number of spread points. The two best performing model types from previous simulations  
 311 were examined; the CGT and the DPM.

312

313 The best performing ANOVA was selected by AIC to include a single significant interaction term. Model type,  
 314 number of points and number of sources all significantly affected the relative performance of the two models  
 315 (ANOVA: model type:  $F_{1,19991}=3693.6$ ,  $p<2e-16$ ; sources:  $F_{2,19991}=2038$ ,  $p<2e-16$ ; points:  $F_{3,19991}=39.1$ ,  $p<2e-16$ ).  
 316 Model type\*sources interaction was also significant ( $F_{4,19991}=222.1$ ,  $p<2e-16$ ). Tukey post-hoc tests at  $\alpha=0.05$

317 showed that the DPM model showed a statistically significant improvement over the CGT algorithm with an effect  
318 size of 4.1% (95% CI: 3.9-4.2%). The MCMC implementation of the DPM outperforms the CGT 67.1% of the time,  
319 and performs as well or better 67.2% of the time. In our simulations this equates to searching on average 410 fewer  
320 cells (95% CI: 394-421) before finding all of the sources.

321

#### 322 **(iv) Case study**

323 The median hit score percentages for the seven vector breeding sites identified in Hassan (2006) were 0.34% for the  
324 DPM model, compared to 0.43% for the CGT and 1.2% for the simple Bayesian model. Note that the hit scores  
325 reported here differ from those in Le Comber et al. (2011), although the surface produced is the same in both cases.  
326 The difference arises because the DPM model uses RgoogleMaps (Loecher 2012), and thus the exact dimensions of  
327 the search area (which affects the hit score) are set by the available zoom levels in the Google Maps data. To allow  
328 direct comparison, we used the same search area for the CGT and the DPM mode.

329

330 For five of the seven sites, hit score percentages for the DPM were less than half a per cent. An additional output of  
331 our model is that it can provide a barplot of the posterior probability of the number of realised sources (Figure 3). In  
332 this case our model indicated the highest probability for seven sources, with a likely range of 6-10. Interestingly,  
333 some of these correspond to areas where no vector species were found by Hassan (2006) (Figure 4). One possibility,  
334 of course, is that these are false-positive results. Alternatively, it is possible that some sources were missed in the  
335 original survey, especially given the often considerable difficulty of locating small, transient breeding populations of  
336 mosquitoes (Carter et al. 2000) and since searches were carried out in a single year (2005), whereas the malaria  
337 cases spanned four (2001-2004) (Hassan 2006; Le Comber et al. 2011).

338

#### 339 **Discussion**

340 Overall the DPM model is an improvement on the existing methods. When the number of sources is greater than one  
341 it outperforms them (Results (i)), it does not require that the number of sources is known *a priori* and, in addition, it  
342 generates estimates of their number. Even in conditions specifically designed to maximise the performance of the  
343 CGT algorithm, the DPM model still obtains a small advantage, reflecting the way in which it appropriately  
344 combines information from observations, rather than taking a simple sum (as in the CGT) or product (as in the

345 simple Bayesian model). The DPM model's analytical method cannot be extended to very large numbers of  
346 observations, but the approach can be implemented in an MCMC algorithm which accurately constructs the  
347 posterior distribution, as demonstrated in Results (ii).

348

349 With these facts established we move on to consider cases in which the DPM model may have a practical advantage  
350 over other approaches. The later set of simulations (Methods (iii) and Results (iii)) demonstrate that there are  
351 biologically plausible settings in which the use of the DPM model can result in an appreciable increase in search  
352 efficiency compared with other methods. Finally, and perhaps most encouragingly, we find that the DPM model  
353 leads to an increase in search efficiency when applied to a real-world data set describing malaria transmission in  
354 Cairo. The improvement over the CGT algorithm is small, but justifies further investigation of this model on a range  
355 of data sets.

356

357 In its construction, the DPM model forms a bridge between the seemingly disparate methodologies of the CGT and  
358 the simple Bayesian approach to geographic profiling. From a practical point of view the major difference between  
359 the two existing approaches lies in whether distributions should be summed (CGT) or multiplied (simple Bayesian).  
360 The DPM model works by splitting the data into groups, with each group corresponding to a different source  
361 location. The laws of probability then dictate that distributions should be multiplied within groups, but summed  
362 between groups. Thus, if all points are assigned to a single source we arrive back at the simple Bayesian model,  
363 while if all points are assigned to different sources we arrive at something more akin to the CGT algorithm. In this  
364 context, our concentration parameter  $\alpha$  can be understood as a prior over the complete spectrum of models, which  
365 allows us to transition between a single-source model and a multiple-source model. When  $\alpha$  is set to zero, the DPM  
366 model becomes mathematically equivalent to the simple Bayesian model; conversely, as  $\alpha$  tends to infinity, we  
367 converge on the CGT algorithm. In the majority of cases – particularly those dealing with biological data – the most  
368 likely explanation for the data will often lie between these two extremes. For example, in the malaria analysis, the  
369 DPM model assigned the highest probability to seven sources from 139 disease case locations (Figure 3).

370

371 In our simulations, the DPM model outperformed both other approaches when there were multiple sources. In cases  
372 with a single source – a common scenario in criminology – the improvement over the CGT, although statistically

373 significant, was minimal when the dispersal distribution was drawn from Equation [1] (when this assumption was  
374 relaxed, the improvement was more marked). The comparison between the DPM model and the simple Bayesian  
375 model shows that latter has a small advantage when there is a single source. However, when there is more than one  
376 source, the DPM shows a large improvement (this is perhaps unsurprising, since the simple Bayesian model assumes  
377 that there is a single source). In real-world applications of GP models it will often (perhaps even always) be the case  
378 that the true number of sources is unknown, therefore the principal advantage of the DPM model lies in its ability to  
379 rigorously handle the problem of multiple sources. In fact, since the difference between the simple Bayesian model  
380 and the DPM model is small when there is a single source, and the advantage offered by the DPM model when there  
381 are multiple sources is larger, we would argue that the DPM model is preferable in real-world applications of GP. In  
382 our simulations, the DPM model outperformed both other approaches in cases with multiple sources. In cases with a  
383 single source – a common scenario in criminology – the improvement over the CGT, although statistically  
384 significant, was minimal when the dispersal distribution was drawn from Equation [1] (when this assumption was  
385 relaxed, the improvement was more marked).

386

387 However, formulating the problem in a rigorous Bayesian framework also allows for a number of useful extensions.  
388 First, our model produces a true probability surface, allowing us to calculate the marginal probability of different  
389 numbers of sources, as in Figure 3. Second, we can produce a probability surface conditional on a particular number  
390 of sources, thereby allowing us to break the overall picture down into different scenarios (we can imagine a different  
391 search strategy, conditional on there being one source, two sources etc.). Third, the DPM model explicitly calculates  
392 the posterior probability under the model that a particular observation is derived from a particular source. This may  
393 be of interest in criminology, where crime linkage is an important problem (Rossmo 2000), and may also be useful  
394 in biological data sets, where the spatial linkage can be validated against other forms of information (for example  
395 genetic data).

396

397 So far, the DPM model is constructed with flexibility in mind, rather than statistical power. For particular cases it  
398 may be possible to increase the power of the model by incorporation of stronger prior information – for example, by  
399 inferring the concentration parameter from training data. Similarly, where empirical evidence has shown that non-  
400 normal dispersal profiles are appropriate (for example, Cauchy distributions in some bird species (Winkler et al.



401 2005; VanHoutan et al. 2007) or bivariate Student's t-distributions in seeds (Nathan & Muller-Landau 2000)), these  
402 can be used within the same general framework.

403

404 As well as producing a range of new outputs, the DPM model could also be extended to incorporate new inputs. For  
405 example, one useful possible extension of our approach is the utilisation of the outputs produced by niche models to  
406 generate priors in the DPM model. Niche modelling is a well-developed field that has recently been placed on a  
407 Bayesian footing (Elith & Leatherwick 2009), making its incorporation into the DPM model relatively  
408 straightforward. A Bayesian niche model produces a probabilistic estimate of the suitability of habitat for the  
409 organism being studied that can be used as a prior in the DPM model. Combining these two approaches would go  
410 some way towards producing a spatially explicit niche model approach, as called for by Peterson et al (2003).

411

412 In epidemiology and invasion biology, much more attention is paid to models that run forwards in time to generate  
413 risk maps or forecasts of future incidence than those that run backwards to locate sources. GP, on the other hand, is  
414 radically different, running backwards in time to use current locations to infer sources (Le Comber & Stevenson  
415 2012). The DPM model structure described above also differs from many spatially explicit epidemiological models,  
416 such as the shot noise Cox process (Møller 2003), in assuming a distribution of point sources, rather than a smoothly  
417 varying hazard function over space. This feature also distinguishes the DPM approach from many existing methods  
418 that are routinely used to detect clusters in ecological and epidemiological data (see Pullan et al. 2012 for a review).  
419 The impact that these different modeling assumptions may have on our conclusions should be explored in further  
420 work. In fact, as O'Leary (O'Leary 2010; O'Leary 2012) has shown, a fully Bayesian implementation of GP can  
421 easily be extended to run forwards in time. Despite the difficulties faced by all predictive models, this could  
422 potentially be important in areas of biology including epidemiology, invasion biology and in conservation biology  
423 (e.g. planning reintroductions of animals or plants).

424

425 The DPM model we present here is a general method that can be applied to data describing spread from common  
426 source. Evidence-based targeting of interventions is a crucial component in the fight against infectious disease, and  
427 targeted interventions are more efficient and more cost-effective than untargeted interventions; for example, malaria  
428 is strongly dependent on the location of vector breeding sites, and most transmission only occurs within short

429 distances of these sites (Carter et al. 2000). Because of this clustering, untargeted intervention is highly inefficient.  
430 In the Cairo study, the DPM model identified five of the seven breeding sites in less than half a percent of the total  
431 search area, representing a dramatic improvement over a non-targeted search.

432

433 Although our implementation of the DPM model can deal with large data sets (>1000 data points), GP methods also  
434 work well with very small data sets (Rossmo 2000; Stevenson et al. 2012), allowing their use in the early stages of  
435 an outbreak or invasion, when control efforts are most likely to be successful. The DPM model provides a useful  
436 practical tool for conservation biologists and epidemiologists, offering improvements over other methods that are  
437 likely to lead to improved targeting of interventions, and more efficient use of resources.

438

#### 439 **Acknowledgements**

440 We would like to thank Ali Hassan for permission to use the malaria data, and the Environmental Criminology  
441 Research Institute (ECRI) Canada for support and useful comments.

442

443

444

445 **References**

446

447 Canter, D., Toby C., Huntley, M., and Missen, C. (2000). Predicting Serial Killers' Home Base Using a Decision

448 Support System. *Journal of Quantitative Criminology*, 16 , 457 – 478.

449

450 Carter. R., Mendis, K., Roberts, D. (2000) Spatial targeting of interventions against malaria. *Bulletin Of The World*451 *Health Organization*, 78, 1401-1411.

452

453 Doney, R. *The aftermath of the Yorkshire Ripper: the response of the United Kingdom Police Service*. In Egger, S.454 A. (1990) *Serial Murder: An Elusive Phenomenon*, Praeger.

455

456 Dorazio, R.M., Mukherjee, B., Zhang, L., Ghosh, M., Jelks, H.L., Jordan, F. (2008) Modelling unobserved sources

457 of heterogeneity in animal abundance using a Dirichlet process prior. *Biometrics*, 64, 635-644.

458

459 el Said, S., Beier, J. C., Kenway, M. A., Morsy, Z. S., Merdan, A. I. (1986) *Anopheles* population dynamics in two460 malaria endemic villages in Faiyum governorate, Egypt. *Journal of the American Mosquito Control Association*, 2.

461

462 Elith, J., Leatherwick, J. R. (2009) Species distribution models: ecological explanation and prediction across space

463 and time. *Annual Review of Ecology, Evolution, and Systematics*, 40, 677-697.

464

465 Ferguson, T. S. (1983) Bayesian density estimation by mixtures of normal distributions. *Recent advances in*466 *statistics*, 287-303.

467

468 Gelman, A., Carlin, J. B., Stern, H. S., Rubin, D. B. (2003) *Bayesian data analysis*, Chapman and Hall/CRC, 2nd

469 Ed.

470

- 471 Green, P. J., Richardson, S. (2001) Modelling heterogeneity with and without Dirichlet process. *Scandinavian*  
472 *Journal of Statistics*, 28, 355-375.
- 473
- 474 Hassan, A. N. (2006) WHO-TDR-SGS, Final report.
- 475
- 476 Huelsenbeck, J.P., Andolfatto, P. (2007) Inference of population structure under a dirichlet process model. *Genetics*,  
477 175, 1787-1802.
- 478
- 479 Huelsenbeck, J.P., Jain, S., Frost, S. W. D., Kosakovsky Pond, S. L. (2006) A Dirichlet process model for detecting  
480 positive selection in protein-coding DNA sequences. *Proceedings of the National Academy of Sciences*, 103, 6263-  
481 6268.
- 482
- 483 Kolar, S.C., Lodge, D. M. (2001) Progress in invasion biology: predicting invaders. *Trends in Ecology and*  
484 *Evolution*, 16, 199-204.
- 485
- 486 Le Comber, S. C., Nicholls, B., Rossmo, D. K., Racey, P. (2006) Geographic profiling and animal foraging. *Journal*  
487 *of theoretical biology*, 240, 223-240.
- 488
- 489 Le Comber, S. C., Rossmo, D. K., Hassan, A. N., Fuller, D. O., Beier, J. C. (2011) Geographic profiling as a novel  
490 spatial tool for targeting infectious disease control. *International journal of health geographics*, 10-35.
- 491
- 492 Le Comber, S. C., Stevenson, M. D. (2012) From Jack the Ripper to epidemiology and ecology. *Trends In Ecology*  
493 *and Evolution*, 27, 307.
- 494
- 495 Levine, N. (1996). Spatial statistics and GIS: Software tools to quantify spatial patterns. *Journal of the American*  
496 *Planning Association*, 62, 381-392.
- 497
- 498 Link, W. A., Eaton, M. J. (2012) On thinning chains in MCMC. *Methods in Ecology and Evolution*, 3, 112-115.

499

500 Loecher, M. (2012) *RgoogleMaps: Overlays on Google map tiles in R*. R package version 1.2.0.2. Berlin School of  
501 Economics and Law. URL <http://CRAN.R-project.org/package=RgoogleMaps>

502

503 Miller, C. (2003) Geographic Profiling Serial Offenses with ECRI's Rigel. *Law Enforcement Technology*, 30, 130-  
504 135.

505

506 Møller, J. (2003) Shot noise Cox processes. *Advances in Applied Probability* 35, 614-640.

507

508 Nathan, R., Muller-Landau, H.C. (2000) Spatial patterns of seed dispersal, their determinants and consequences for  
509 recruitment. *Trends In Ecology and Evolution*, 15, 278–285.

510

511 Neal, R.M. (2000) Markov chain sampling methods for Dirichlet Process mixture models. *Journal of computational  
512 and graphical statistics*, 9, 249-265.

513

514 O'Leary, M. (2009) The mathematics of geographic profiling. *Journal of Investigative Psychology and Offender  
515 Profiling*, 6, 253-265.

516

517 O'Leary, M. (2010) Implementing a Bayesian approach to criminal geographic profiling. *First International  
518 Conference on Computing for Geospatial Research and Application*, June 21-23 Washington, D.C.

519

520 O'Leary, M. (2012) *New Mathematical Approach to Geographic Profiling*, National Insitute of Justice, Washington,  
521 D.C.

522

523 Peterson, A. T. (2003) Predicting the geography of species' invasions via ecological niche modeling. *The Quarterly  
524 Review of Biology*, 78, 419–433.

525

- 526 Pullan, R. L., Sturrock, H. J. W., Magalhaes, R. J. S. et al. (2012) Spatial parasite ecology and epidemiology: a  
527 review of methods and applications. *Parasitology* 139, 1870-1887.  
528
- 529 R Core Team (2012) *R: A language and environment for statistical computing*. R Foundation for Statistical  
530 Computing, Vienna, Austria. URL <http://www.R-project.org/>[accessed 20 November 2012]  
531
- 532 Raine, N. E., Rossmo, D. K., Le Comber, S.C. (2009) Geographic profiling applied to testing models of bumble-bee  
533 foraging. *Journal of the Royal Society*, 6, 307-319.  
534
- 535 Rossmo, D.K., *Geographic profiling: Target patterns of serial murderers*, Unpublished doctoral dissertation, Simon  
536 Fraser University, Burnaby, BC, Canada.  
537
- 538 Rossmo, D. K. (1993) A methodological model. *American Journal of Criminal Justice*, 17, 1-21.  
539
- 540 Rossmo, D. K. (2000) *Geographic Profiling*. CRC Press 1st Ed, New York.  
541
- 542 Snook, B., Canter, D., & Bennell, C. (2002) Predicting the home location of serial offenders: A preliminary  
543 comparison of the accuracy of human judges with a geographic profiling system. *Behavioral Sciences & the Law*,  
544 20, 109-118.  
545
- 546 Snook, B., Taylor, P. J., and Bennell, C. (2005) Shortcuts to Geographic Profiling success: A reply to Rossmo  
547 (2005). *Applied Cognitive Psychology*, 19, 655-661  
548
- 549 Stevenson, M. D., Rossmo, D. K., Knell, R. J., Le Comber, S. C. (2012) Geographic profiling as a novel spatial tool  
550 for targeting the control of invasive species. *Ecography*, 10, 704-715.  
551
- 552 Van Houtan, K.S., Pimm, S. L., Halley, J. M., Bierregaard, R. O. Jr., Lovejoy, T. E. (2007) Dispersal of Amazonian  
553 birds in continuous and fragmented forest. *Ecology Letters*, 10, 219-229.

554

555 Winkler, D. W., Wrege, P. W., Allen, P. E., Kast, T. L., Senesac, P., Wasson, M. F., Sullivan, P. J. (2005) The natal

556 dispersal of tree swallows in a continuous mainland environment. *Journal of Animal Ecology*, 74,1080–1090.

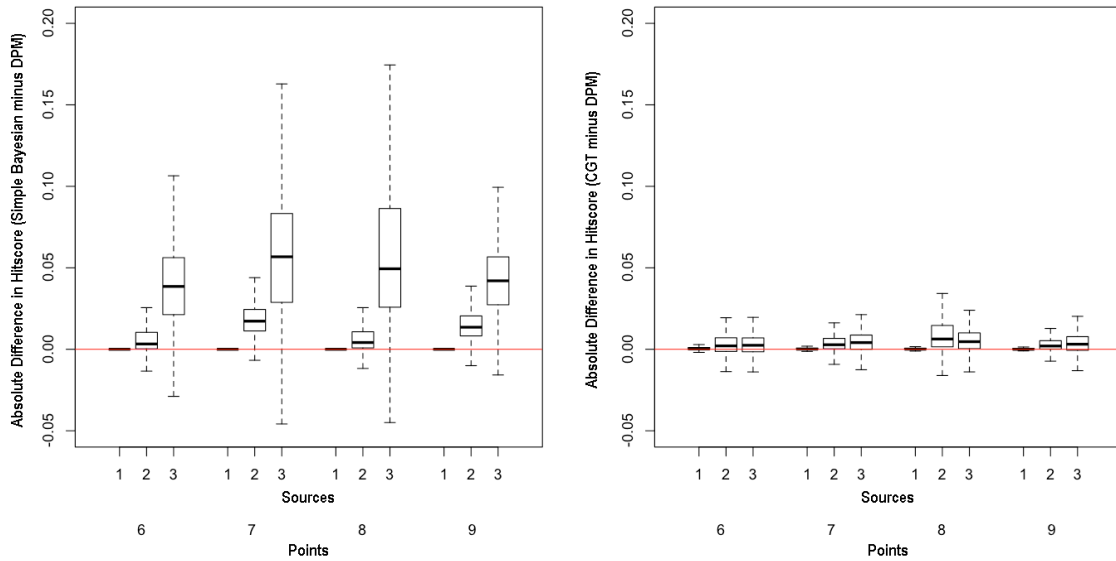
557

558

559

560 **Figures**

561

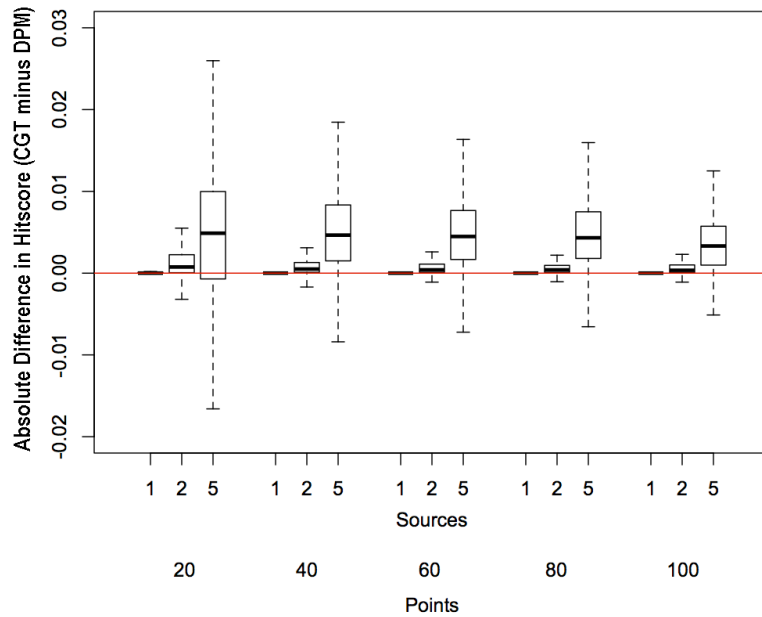


562

563 **Figure 1** Comparison of the analytical form of the DPM model against (A) the simple Bayesian model, and (B) the  
 564 CGT algorithm, expressed as the hit score percentage of the simple Bayesian model minus the hit score percentage  
 565 of the DPM model, and the hit score percentage of the CGT algorithm minus the hit score percentage of the DPM  
 566 model, respectively. Thus, points above the red line indicate cases in which the DPM model outperformed the other  
 567 models. In both cases, the DPM model has a statistically significant advantage, although this is more pronounced for  
 568 the comparison with the simple Bayesian model. In both comparisons, the relative performance of the DPM model  
 569 improves as number of sources increases.

570





571

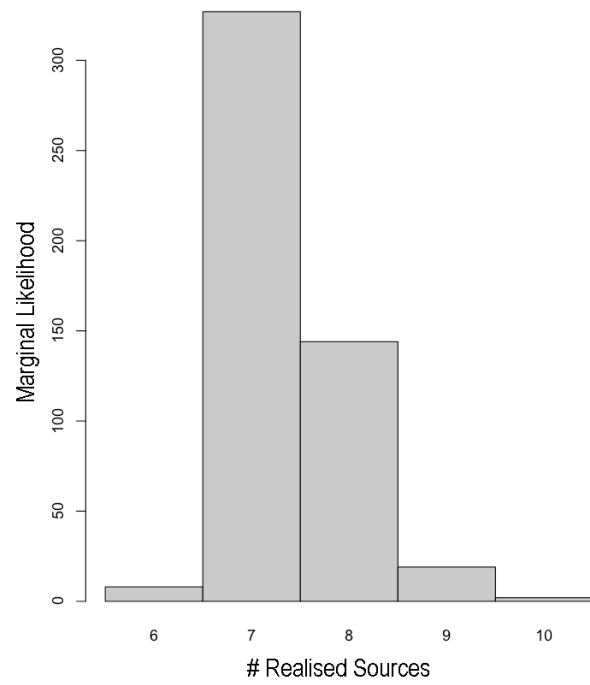
572 **Figure 2** Comparison of the MCMC implementation of the DPM model against the CGT algorithm, expressed as

573 the hit score percentage of the CGT algorithm minus the hit score percentage of the DPM model. Again, points

574 above the red line indicate cases in which the DPM model outperformed the other model. The DPM model

575 outperformed the CGT algorithm, especially as number of sources increases.

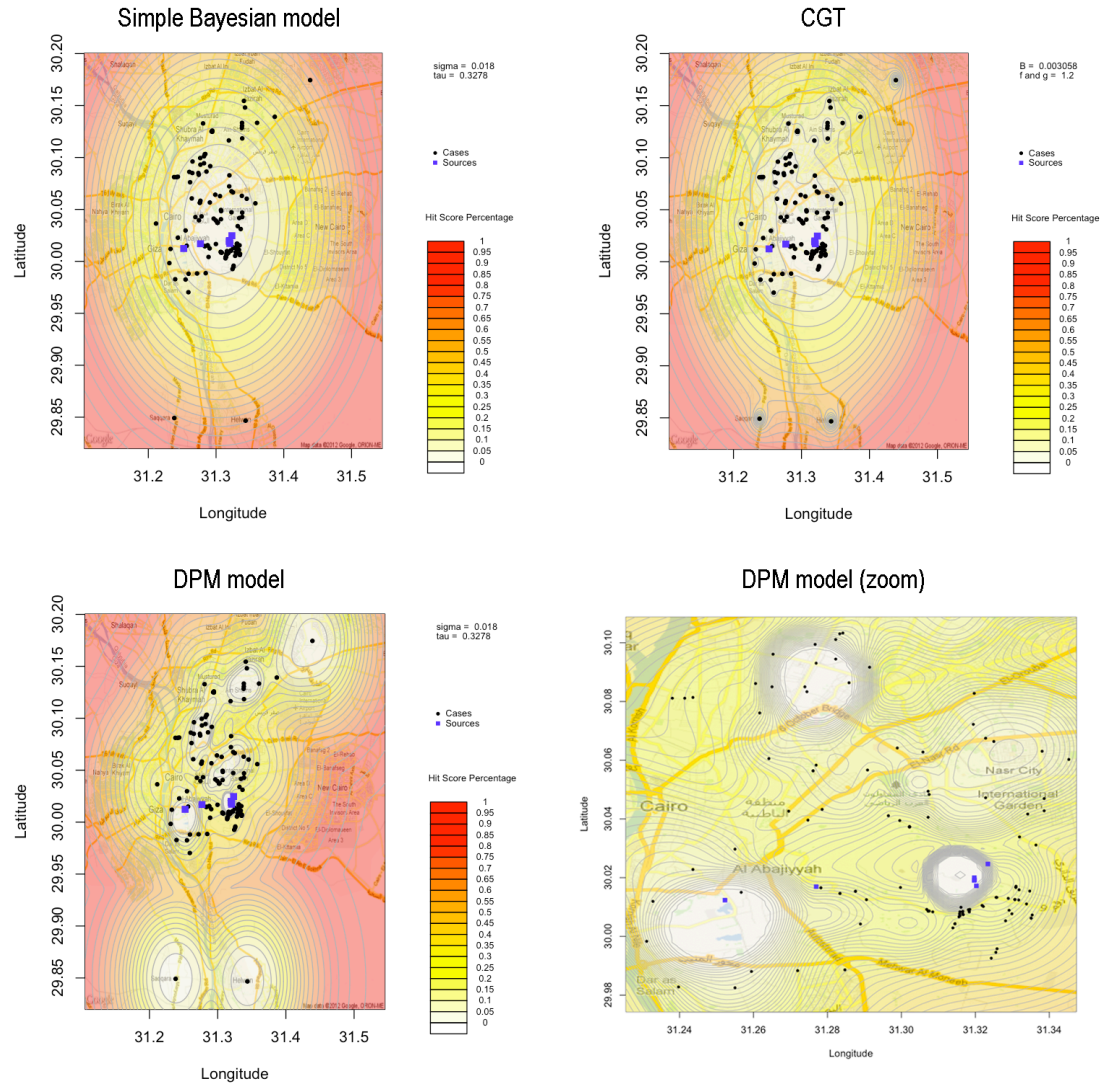
576



577

578 **Figure 3** Marginal likelihood of different numbers of realised infection sources for the Cairo data. The DPM model  
579 estimates that there are 6-10 sources, and assigns the highest likelihood to seven sources.

580



581

582 **Figure 4** Geoprofile from 139 *Plasmodium vivax* cases in Cairo, Egypt, using (A) the simple Bayesian model; (B)

583 the CGT algorithm; (C) the DPM model. (D) shows a close-up of the DPM surface. In all cases the observed data

584 points are shown as black circles, while the empirically identified sources are shown as blue squares.